



Properties of Zinc Oxide Nanowires by Hybrid Microwave-Assisted Sonochemical Technique: Effects of Different Zinc Salts as Precursor

Maryam Mohammad^{1,2,3}, Mohd Firdaus Malek^{1,2}, Nurul Zulaikha Mohammad Zamri^{1,2}, Noor Fatin Sofea Zulkifli^{1,2}, Mohamad Dzulfiqar Bakri^{1,2}, Nur Fairuz Rostan^{1,2}, Nurfatini Atiqrah Khairul Azhar^{1,2}, Zahidah Othman^{1,2}, Mohamad Hafiz Mamat⁴, Zuraida Khusaimi^{1,2}, Ruziana Mohamed^{1,2} and Mohamad Rusop Mahmood^{1,4}*

¹NANO-SciTech Lab (NST), Centre for Functional Materials and Nanotechnology (FMN), Institute of Science (IOS), Universiti Teknologi MARA (UiTM), 40450 Shah Alam, Selangor, Malaysia.

²School of Physics and Materials Studies, Faculty of Applied Sciences, Universiti Teknologi MARA (UiTM), 40450 Shah Alam, Selangor, Malaysia.

³School of Physics and Materials Studies, Faculty of Applied Sciences, Universiti Teknologi MARA (UiTM) Perak Branch, Tapah Campus, 35400 Tapah Road, Perak, Malaysia.

⁴NANO-ElecTronic Centre (NET), School of Electrical Engineering, College of Engineering, Universiti Teknologi MARA (UiTM), 40450 Shah Alam, Selangor, Malaysia.

Abstract

The key material, namely precursor has a significant impact on the synthesis condition of zinc oxide (ZnO) nanomaterials production. Thus, solution synthesis methods using simple salts as precursors, specifically zinc acetate dehydrate (ZA) and zinc nitrate hexahydrate (ZN), have become a preferred bottom-up synthesis route for metals/metal oxides because they allow for enhancement of growth parameters of the ZnO nanomaterials. In our study, zinc oxide nanowires (ZnO NWs) have been successfully synthesized via a novel hybrid microwave-assisted sonochemical technique (HMAST) where different precursor of zinc salts was used specifically zinc acetate dihydrate and zinc nitrate hexahydrate at optimized parameters of 12.5 mM solution concentration, 600 W microwave power, and a rapid deposition time of 60 minutes. The effect of different precursors on the morphological, structural, and optical properties of the ZnO NWs has also been studied. The results of field emission scanning electron microscope (FESEM) images of the ZnO NWs from both precursors indicate that ZA is more favorable as a precursor as compared to ZN as it produces a higher quality of aligned ZnO NWs which is more uniformly distributed with even sizes and smaller average diameter size of ~28.44 nm. Whereas the X-ray Diffraction (XRD) pattern of ZnO NWs grown from ZA as precursor has stronger and narrower peaks at (002) orientation as compared to the ZnO NWs produced by ZN as a precursor with calculated crystallite size of ~26.87 nm and ~33.33 nm respectively. The optical transmittance recorded from the Ultraviolet-visible (UV-Vis) spectrometer also presents a higher average transmittance of 95.29 % when using ZA as a precursor as opposed to ZN which displays a slightly lower transmittance of an average of 93.32 % over the same wavelength.

Keywords: Zinc oxide nanowires, Precursor, Zinc acetate, Zinc nitrate, Microwave-assisted

Full length article *Corresponding Author, e-mail: mfmalek07@uitm.edu.my; mfmalek07@gmail.com

1. Introduction

The study and development of oxide-based multifunctional materials and one-dimensional

nanostructures had been ongoing for decades where one of the most popular oxide materials is zinc oxide nanostructures

due to their unique and superior properties. Advantages of this material had been reported to enhance the performances of electric and electronic devices, optoelectronics applications, photocatalysis, sensors, and many more [1-3].

The most popular method in synthesizing these materials would be solution-based synthesis techniques to create a broad variety of 1D nanometer to micrometre ZnO NSs such as rods, plates, tubes, rings, tetrapods, prisms, pyramids, spheres, hollow structures, flowerlike, and multineedle-shaped crystals [4-6]. ZnO nanowires (ZnO NWs) were particularly notable among other nanostructures due to their quasi one-dimensional (1-D) architectures displaying quantum confinement phenomena and huge surface to volume ratios. It can be thought of as a 1-D channel with electron, hole, and photon absorption, emission, and transport, resulting in strong confinement effects on the carriers and photons, resulting in various new optical and electrical properties for device applications [7-9]. Furthermore, it has been discovered that one-dimensional nanostructures (NSs), like nanowires grown on a substrate, offer a larger surface-to-volume ratio than nanoparticles (NPs) deposited on a flat surface and, as a result, a higher photocatalytic activity through enhanced adsorption of target organic molecules onto the catalyst surface [10].

Other benefits include a large selection of substrate materials and geometries, as well as its straightforward crystal-growth process, which offers noticeably cheaper production costs than other semiconductors utilized in nanotechnology [11-12]. The nanowires formation was also aimed specifically due to its hexagonal wurtzite structure of ZnO which is the most thermodynamically stable and hence most common among the three structures, i.e., wurtzite, zincblende, and rock salt [13-14]. The substance utilized as a precursor will also have a significant impact on the synthesis conditions of ZnO NSs production. Previous research has revealed that controlled synthesis of materials at the micro- and nanoscale has been of research interest while being faced with numerous difficulties since the physical and chemical characteristics and functionalities of a specific material are determined by its structure and/or morphology. Therefore, bottom-up solution synthesis techniques using alkoxides or simple salts as precursors, particularly zinc acetate dehydrate (ZA) and zinc nitrate hexahydrate (ZN), have gained popularity because they enable fine-tuning of growth parameters like solution composition, chemistry, temperature, reactant concentration, reaction rate, and solubility, which are intricately linked and collectively influence the parameters of crystal growth [15-17].

This is supported in the study done by Liang et al. whereby both materials are known to result in the formation of wurtzite-structured, twinned hexagonal rods of ZnO NSs [18]. The conventional method of producing ZnO NWs by solution-based approach, however, mainly does not emphasize on the solution preparation process but focused more on the effects of stabilizer instead of the reactant dispersion which caused non-homogeneous reaction during the mixing process of precursor and solvent will contribute to the formation of a large particles size and reduce the surface area of the nanostructures. Through defects states such as grain boundaries, this behavior will lead to limited electron transport and high recombination [19]. Additionally, though these prevalent growth methods for ZnO NWs currently practiced are mostly successful that is chemical and physical

techniques like thermal evaporation, chemical vapor deposition (CVD) and cyclic feeding CVD, sol-gel deposition, electrochemical deposition, hydrothermal and solvothermal growth as well as surfactant and capping agents-assisted growth, they do have a few drawbacks, such as low productivity or severe impurities from their employed assistant, also known as a catalyst or precursor, which can cause complications for their actual nanodevice application [20-30]. Another downside is that using these methods involves harsh circumstances including extreme heat and pressure, pricey materials, and complicated processes. To overcome these concerns, microwave-assisted techniques had been proposed as an alternative. Microwave comprises the region of the electromagnetic spectrum that has a wavelength (λ) between 1 mm and 1 m, which is equivalent to a frequency range between 300 MHz ($\lambda = 1$ m) and 300 GHz ($\lambda = 1$ mm) [31-32]. Microwave technology itself has several advantages, including scalability, low energy consumption, rapid expansion, cheap cost, and ease of handling, making it a highly lauded technique to address these issues [33-35]. Furthermore, the microwave-assisted technique offers greater control over the structure and dimensional dispersion of ZnO NSs than a more conventional way of ZnO NS synthesis [36]. As a result, experimental results are guaranteed to be more consistent. Additionally, microwave irradiation is essential for chemical processes that take place in aqueous media, decrease the amount of production time and cost, decreasing the particle size with a narrow size distribution, increasing the product yield rate, and generating high-purity products in comparison to conventional methods [37-42]. Thus, our research intends to optimize the aforementioned method by introducing our very own Hybrid Microwave-Assisted Sonochemical Technique (HMAST) which incorporates a very effective and often employed solution-based method whereby the sonification was incorporated during the mixing process, to significantly improve the interaction between the precursor and stabilizing agent and thus provide better overall control of the features of the nanostructure and further assisted by microwave irradiation to expedite the production process while also studying the effect of different zinc salts namely ZA and ZN as precursor on the properties of ZnO NWs produced.

2. Materials and methods

The research methodology comprises three different phases as summarized. The first process would be the preparation and cleaning of the glass substrates. Then the preparation of ZnO NPs thin film using ultrasonic-assisted sol-gel spin coating technique producing ZnO NPs array. It will then undergo a deposition process in the microwave to produce ZnO NWs. Analysis of data was done to investigate the morphological structures of the samples by using Field Emission Scanning Electron Microscope (FESEM, JEOL JSM-7600F), X-ray Diffraction (XRD) (XRD, PANalytical X'Pert PRO) and Ultraviolet-visible (UV-Vis) spectrometer (Cary 5000).

2.1. Preparation of ZnO nanoparticles Seeded Layer Thin films

Zinc Oxide-Based Nanoparticles were prepared as a seed layer of thin films on a glass substrate which was deposited by an optimized ultrasonic-assisted sol-gel (sonochemical) spin-coating technique [43-44]. The sonicated sol-gel ZnO

was prepared by dissolving 0.4 M zinc acetate dehydrates $[(\text{Zn}(\text{CH}_3\text{COO})_2 \cdot 2\text{H}_2\text{O})]$; Merck] which acts as the precursor in the solvent of 2-methoxy ethanol $[\text{C}_3\text{H}_8\text{O}_2]$; Merck] at room temperature.

Then, 1 at% of aluminum nitrate nonahydrate $[\text{Al}(\text{NO}_3)_3 \cdot 9\text{H}_2\text{O}]$; Analar] and 0.4 monoethanolamines [MEA, $\text{C}_2\text{H}_7\text{NO}$; R&M] were added into the solution as dopant and stabilizer respectively. The molar ratio of MEA to zinc acetate dehydrate was maintained at 1:1, and the resultant solution was stirred at 80 °C for 40 minutes to yield a clear and homogeneous solution. Afterward, the solution was sonicated at 50°C for 30 minutes using an ultrasonic water bath (Hwasin Technology Powersonic 405, 40kHz) and cooled to room temperature. The solution will then be used to coat the glass substrate using the spin coating technique where 10 drops of the solution were deposited onto the substrate at a speed of 3000 rpm for 30 s. Lastly, the samples were preheated in an atmosphere ambient at 300°C for 10 minutes to remove solvent and the deposition processes were repeated for the second to the fifth layer of film to achieve the required film thickness. All samples were annealed in a furnace at a temperature of 500°C for 1 hour.

2.2. Deposition of ZnO Nanostructures via Microwave-Assisted Sonochemical Technique

ZnO NWs were grown via the novel HMAST method. An optimized 12.5 mM concentration of the solution was prepared at 1:1 ratio of Zinc acetate dehydrates $[\text{Zn}(\text{CH}_3\text{COO})_2 \cdot 2\text{H}_2\text{O}]$; Merck] and hexamethylenetetramine [HMTA, $\text{C}_6\text{H}_{12}\text{N}_4$; Merck] which acts as the precursor and stabilizer, respectively [45]. The reagents were dissolved and reacted in a beaker filled with 1000 mL distilled water as a solvent and stirred at 80 °C for 30 minutes to yield a clear and homogeneous solution. Next, the solution was sonicated at 50 °C for 30 minutes using an ultrasonic water bath (Hwasin Technology Powersonic 405, 40 kHz). The solution was then aged at room temperature for 1 hour and poured into a Schott bottle of 250 ml volume capacities where the optimized seed layer-coated glass substrates were placed at the bottom of the container. Afterward, the container was placed inside the 2.45 GHz microwave (SHARP 25L Microwave Oven R352ZS) which was set to a microwave power 600 Watt for 60 minutes. Once done, the samples were annealed at a temperature of 500 °C for 1 hour. The whole process is then repeated by substituting the zinc acetate dehydrate with zinc Nitrate hexahydrate $(\text{Zn}(\text{NO}_3)_2 \cdot 6\text{H}_2\text{O})$ as the precursor. The procedures described above are depicted in **Figure 1**.

2.3. Characterization method

The structural and morphological properties were characterized by X-ray diffraction (XRD, PANalytical X'Pert PRO) with Cu K-alpha radiation of a wavelength of 1.54 Å and field emission scanning electron microscope (FESEM, JEOL JSM-7600F). The optical properties were characterized by UV-visible spectroscopy (UV-Vis, Cary 5000).

3. Results and Discussions

3.1. Morphological and Structural Study

Figure 2 shows the top view of the ZnO NWs created using the HMAST approach at different precursor of zinc acetate (**Fig. 2a**) and zinc nitrate (**Fig. 2b**). It is evident from both samples that ZnO NSs were successfully produced in

nanowire-type of formation at the surface of the glass substrate within a very brief period of deposition time of 60 minutes which may be attributed to microwave chemistry, as discussed by Abu ul Hassan et al., where microwave heating provides homogeneous heat transfer to the solution mixture for chemical reactions, thereby speeding up the synthesis process [46]. Although the produced ZnO NWs on both samples have a distinct hexagonal wurtzite structure and are vertically oriented and tightly packed onto the substrate, it can be clearly seen that ZnO NWs from ZA is more uniformly distributed with even sizes of nanowires as compared to ZnO NWs by ZN. This is consistent with the findings of Rani et al. who used a comparable hydrothermal synthesis technique and deposition solution concentration and observed that the ZnO NSs samples that were displayed were distributed uniformly when using ZA as the precursor as opposed to when using ZN, where the ZnO NRs had begun to embed one another [47].

The synthesized ZnO NWs from ZA also have an average diameter of ~28.44 nm which is smaller than when the precursor was changed to ZN with an average diameter of ~38.76 nm diameter of ZnO NWs which may also be caused by the acidic strength of zinc nitrate, according to Singh et al., who found that the different morphologies of zinc oxide obtained are due to variations in crystal growth rates relating to different crystallographic planes, where the acidic strength of the zinc oxide precursors used in these studies are as follows: nitrate > acetate, where the sample generated by the less acidic ZA had flat-ended hexagonal prisms that were longer than those produced by the more acidic ZN. Additionally, it will produce bigger linked particles or structures at the same time [48-49]. **Figure 3** shows The X-ray diffraction (XRD) spectra of the ZnO NWs produced by the HMAST method using different precursors of zinc acetate dehydrate (**Fig. 3a**) and zinc nitrate hexahydrate (**Fig. 3b**) The indexing of the various XRD peaks was carried out in accordance with the Joint Committee on Powder Diffraction Standards (JCPDS) standard database of ZnO hexagonal structure (File No 36-1451). The ZnO NWs produced from both samples are highly crystalline having hexagonal wurtzite structure with preferable c-axis orientation as well as exhibiting six clear diffraction peaks recorded between 20° to 60°. These peaks were indexed at (100), (101), and (002) with the highest intensity and lower at (102), (110), and (112) planes.

Fig. 3 (a) had also shown that XRD pattern of ZnO NWs grown from ZA as precursor has stronger and narrower XRD peaks at (002) orientation as compared to the ZnO NWs produced by ZN as a precursor with calculated crystallite size of ZnO NWs from ZA of ~26.87 nm and ZnO NWs from ZN with ~33.33 nm crystallite size which is similar to the diameter size of grown nanowires respectively. Furthermore, the great intensity of the ZnO NWs within the c-axis direction from the ZA precursor could be attributed to the nearly perfect alignment of the nanowires. It was outlined in the work by Akgun et al. on how zinc acetate dihydrate makes it possible to synthesize nanowires with the largest aspect ratio and longest length, resulting in improved alignment and a predominance of the steric hindrance effect. As a result, the unit volume for diffraction increases, and the peak intensity does as well [50].

3.2. Optical properties

At room temperature, UV-VIS spectrometer measurements between 200 and 800 nm are used to characterize the optical characteristics of the produced ZnO NWs.

All synthetic ZnO samples have optical absorption spectra in the visible and ultraviolet ranges that show a movement of the absorption band edge into the visible region and its dependency on the precursor. The transmittance spectra of the ZnO NWs produced by the HMAST technique at various precursors, including zinc acetate dehydrate (Fig. 4a) and zinc nitrate hexahydrate (Fig. 4b), are presented in Figure 4. In the whole visible region, the transmittance spectra show an exciton peak in the 350–380 nm range and reduced absorbance above 380 nm. Sharp absorption edges

suggest smaller ZnO particle sizes, while strong absorbance in the UV range suggests superior crystallinity [51].

The optical transmittance is calculated within the wavelength from 400 and 800 nm where higher transmittance was recorded for the sample synthesized using ZA precursor with average transmittance of 95.29 % whereas the sample using ZN precursor shows slightly lower transmittance of an average 93.32 % over the same wavelength. In general, both samples displayed excellent transparency, and it is widely known that electrical devices can benefit from strong transmittance qualities by using them, for example, in the window layer of solar cells, to catch the most photons.

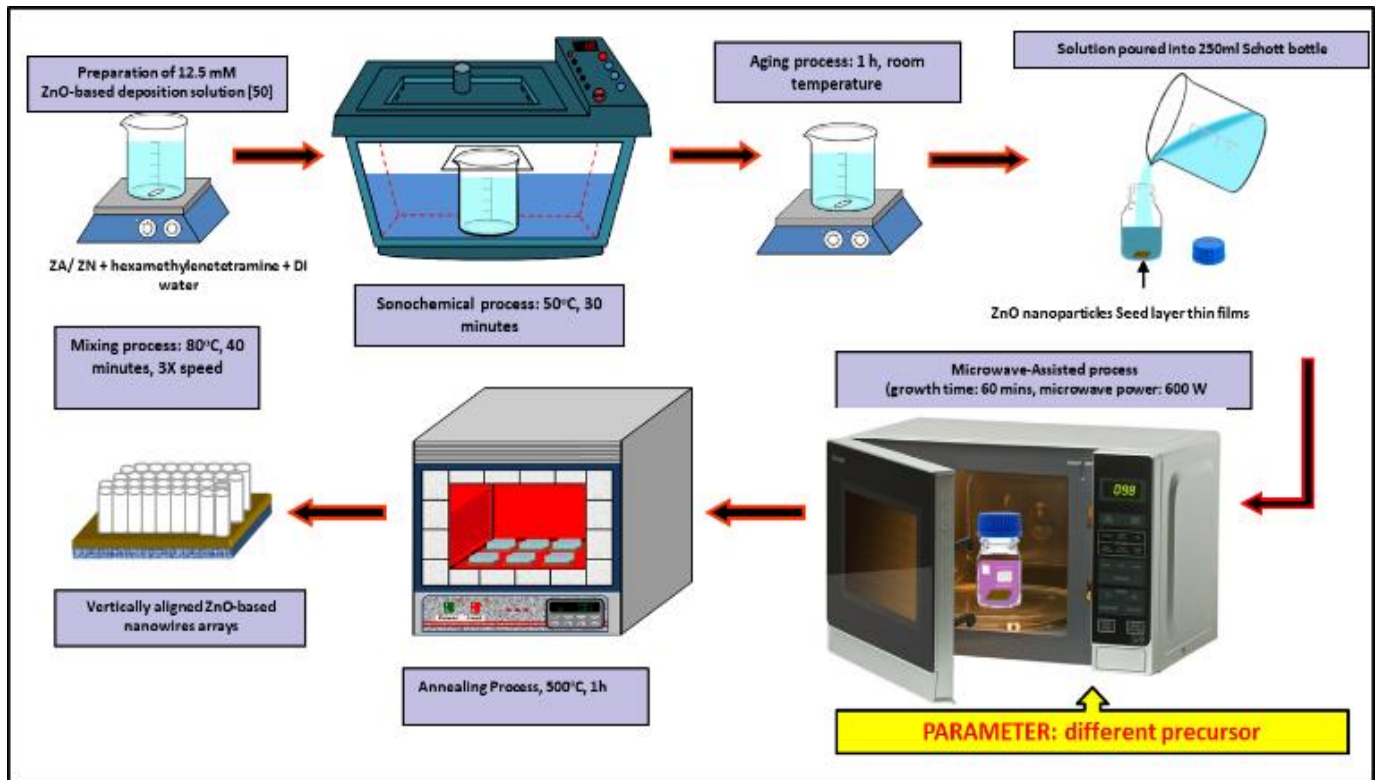


Fig 1: Schematic Diagram on the Deposition of ZnO NWs via HMAST

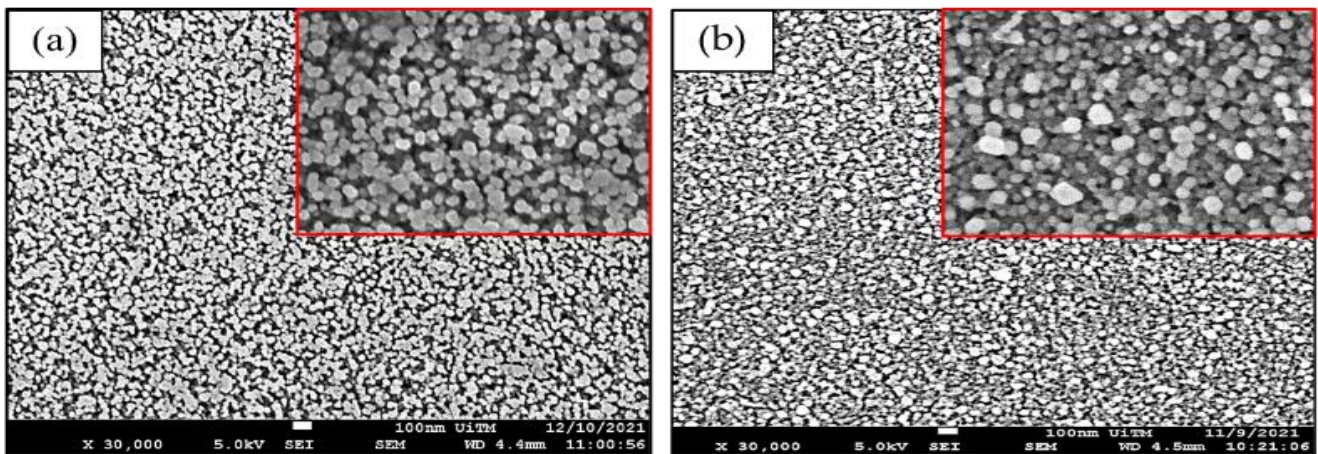


Fig 2: FESEM images (30k and 100k magnification) of ZnO NWs by HMAST method at different precursors of (a) ZA and (b) ZN

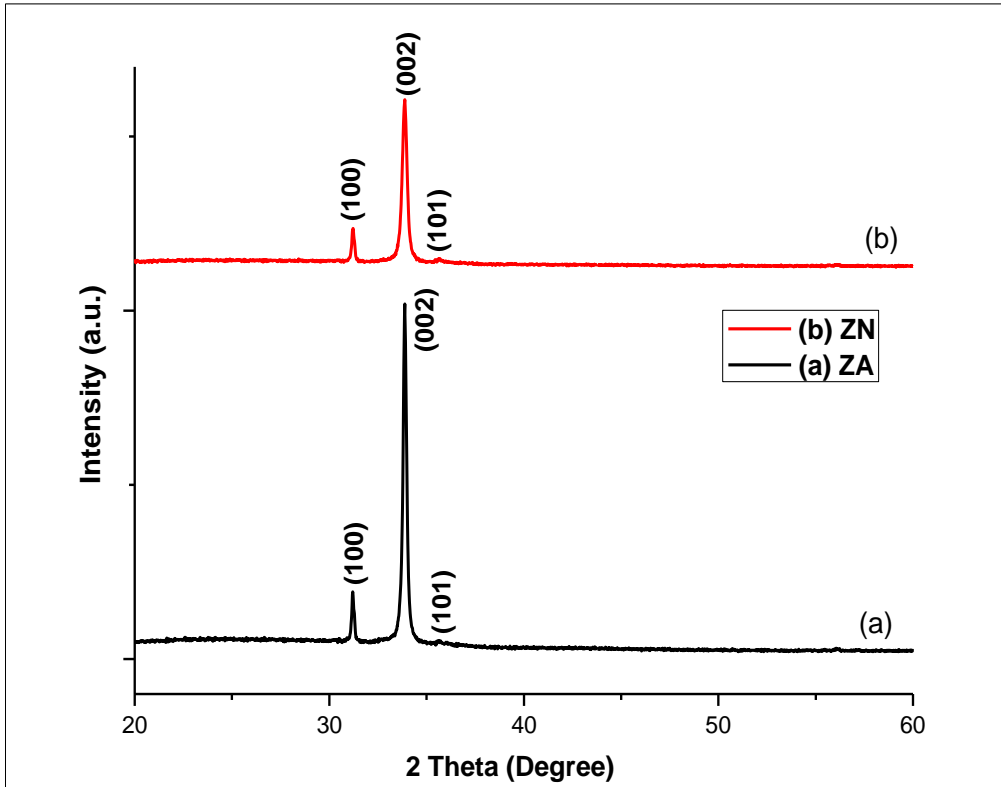


Fig 3: XRD spectra of ZnO NWs by HMAST method at different precursors of (a) ZA and (b) ZN

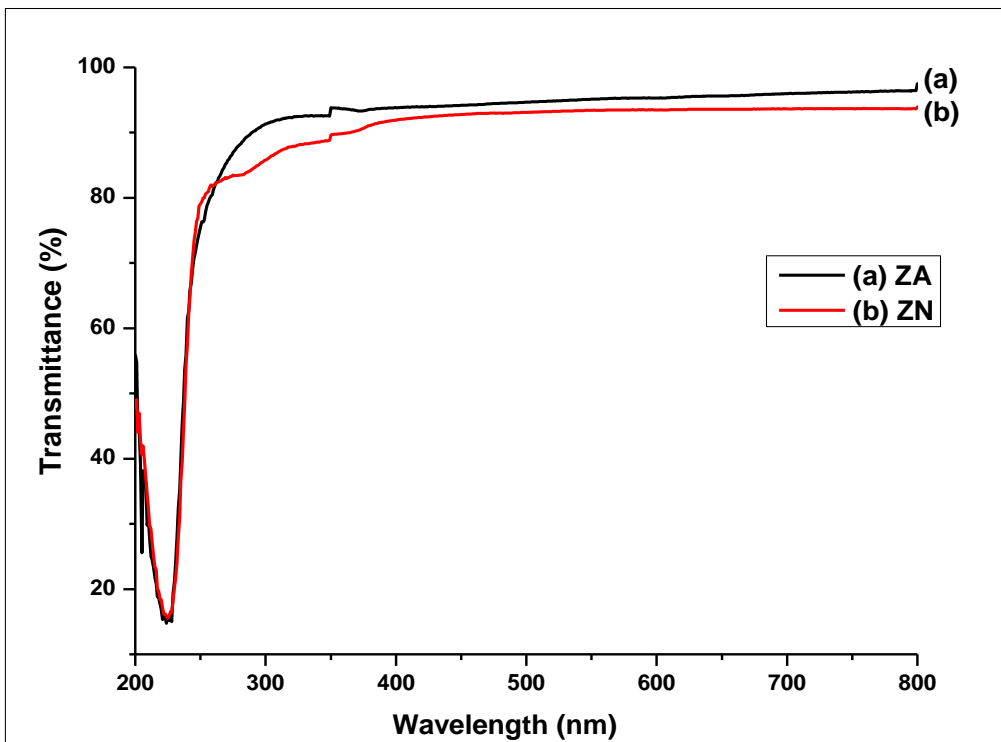


Fig 4: UV-VIS Transmittance spectra of ZnO NWs by HMAST method at different precursors of (a) ZA and (b) ZN

4. Conclusions

It can be concluded that highly crystalline ZnO NWs with a hexagonal wurtzite structure and a preferred c-axis orientation were successfully synthesized using a novel hybrid microwave-assisted sonochemical technique at an optimized microwave power of 600 W with 12.5 mM concentration and 60 minutes of deposition time with the variable precursor of zinc acetate dehydrate and zinc nitrate hexahydrate. Higher purity and uniformity of the aligned ZnO NWs generated are shown by the stronger and narrower (002) XRD peak intensities of the ZnO NWs from ZA as compared to ZN as the precursor. This conclusion was further corroborated by FESEM images of the samples, which show reduced wire diameters when employing ZA as a precursor and smaller crystallite sizes when compared to ZnO NWs by ZN. This is further substantiated by the UV-VIS transmittance spectra, which demonstrated that ZnO NWs made using this approach have greater transmittance when employing ZA as a precursor.

Acknowledgment

This work was supported by Grant No. 600-RMC/YTR/5/3 (005/2021) under the Ministry of Higher Education (MOHE) and the Universiti Teknologi MARA (UiTM), Malaysia. The authors would like to thank Ms. Irmaizatussyehdany Buniyamin (Senior Research Officer), Mr. Muhammad Faizal Abd Halim (Assistant Research Officer), Mr. Salifairus Mohammad Jafar (UiTM Senior Science Officer), and Mr. Mohd Azlan Jaafar (UiTM Assistant Engineer) for their kind help and support of this research.

References

- [1] M. T. Noman, N. Amor, & M. Petru. (2022). Synthesis and applications of ZnO nanostructures (ZONSS): A review. *Critical Reviews in Solid State and Materials Sciences*. 47 (2): 99-141.
- [2] P. Rong, S. Ren, & Q. Yu. (2019). Fabrications and applications of ZnO nanomaterials in flexible functional devices-a review. *Critical reviews in analytical chemistry*. 49 (4): 336-349.
- [3] J. Theerthagiri, S. Salla, R. A. Senthil, P. Nithyadharseni, A. Madankumar, P. Arunachalam, ... & H. S. Kim. (2019). A review on ZnO nanostructured materials: energy, environmental and biological applications. *Nanotechnology*. 30 (39): 392001.
- [4] A. A. Ghassan, N. A. Mijan, & Y. H. Taufiq-Yap. (2019). Nanomaterials: an overview of nanorods synthesis and optimization. *Nanorods and nanocomposites*. 11 (11): 8-33.
- [5] M. S. Lv, C. Li, Y. N. Li, X. F. Zhang, Z. P. Deng, X. L. Cheng, ... & S. Gao. (2023). Facilely controlled synthesis of porous ZnO nanotubes with rich oxygen vacancies for highly sensitive and selective detection of NO₂ at low temperature. *Sensors and Actuators B: Chemical*. 375: 132865.
- [6] M. Hong, J. Meng, H. Yu, J. Du, Y. Ou, Q. Liao, ... & Y. Zhang. (2021). Ultra-stable ZnO nanobelts in electrochemical environments. *Materials Chemistry Frontiers*. 5 (1): 430-437.
- [7] A. Galdámez-Martinez, G. Santana, F. Güell, P. R. Martínez-Alanis, & A. Dutt. (2020). Photoluminescence of ZnO nanowires: a review. *Nanomaterials*. 10 (5): 857.
- [8] C. V. Manzano, L. Philippe, & A. Serrà. (2022). Recent progress in the electrochemical deposition of ZnO nanowires: Synthesis approaches and applications. *Critical Reviews in Solid State and Materials Sciences*. 47 (5): 772-805.
- [9] R. Mardosaite, A. Jurkeviciute, & S. Rackauskas. (2021). Superhydrophobic ZnO nanowires: Wettability mechanisms and functional applications. *Crystal Growth & Design*. 21 (8): 4765-4779.
- [10] Y. Zhang, M. K. Ram, E. K. Stefanakos, & D. Y. Goswami. (2012). Synthesis, characterization, and applications of ZnO nanowires. *Journal of Nanomaterials*. 2012: 1-22.
- [11] S. Baruah, R. F. Rafique, & J. Dutta. (2008). Visible light photocatalysis by tailoring crystal defects in zinc oxide nanostructures. *Nano*. 3 (05): 399-407.
- [12] Q. Zhou, J. Z. Wen, P. Zhao, & W. A. Anderson. (2017). Synthesis of vertically-aligned zinc oxide nanowires and their application as a photocatalyst. *Nanomaterials*. 7 (1): 9.
- [13] Ü. Özgür, Y. I. Alivov, C. Liu, A. Teke, M. A. Reshchikov, S. Doğan, ... & A. H. Morkoç. (2005). A comprehensive review of ZnO materials and devices. *Journal of applied physics*. 98 (4).
- [14] A. Moezzi, A. M. McDonagh, & M. B. Cortie. (2012). Zinc oxide particles: Synthesis, properties and applications. *Chemical engineering journal*. 185: 1-22.
- [15] S. Shankar, & J. W. Rhim. (2019). Effect of Zn salts and hydrolyzing agents on the morphology and antibacterial activity of zinc oxide nanoparticles. *Environmental Chemistry Letters*. 17: 1105-1109.
- [16] Rajamanickam, S., Mohammad, S. M., & Hassan, Z. (2020). Effect of zinc acetate dihydrate concentration on morphology of ZnO seed layer and ZnO nanorods grown by hydrothermal method. *Colloid and Interface Science Communications*. 38: 100312.
- [17] E. Y. Shaba, J. O. Jacob, J. O. Tijani., & M. A. T. Suleiman. (2021). A critical review of synthesis parameters affecting the properties of zinc oxide nanoparticle and its application in wastewater treatment. *Applied Water Science*. 11:1-41.
- [18] M. K. Liang, M. J. Limo, A. Sola-Rabada, M. J. Roe, & C. C. Perry. (2014). New insights into the mechanism of ZnO formation from aqueous solutions of zinc acetate and zinc nitrate. *Chemistry of Materials*. 26 (14): 4119-4129.
- [19] M. A. Messih, M. A. Ahmed, A. Soltan, & S. S. Anis. (2019). Synthesis and characterization of novel Ag/ZnO nanoparticles for photocatalytic degradation of methylene blue under UV and solar irradiation. *Journal of Physics and Chemistry of Solids*. 135: 109086.

- [20] T. Van Khai, V. M. Thanh, & T. Dai Lam. (2018). Structural, optical and gas sensing properties of vertically well-aligned ZnO nanowires grown on graphene/Si substrate by thermal evaporation method. *Materials Characterization*. 141: 296-317.
- [21] H. Ahmoum, G. Li, S. Belakry, M. Boughrara, M. S. Su'ait, M. Kerouad, & Q. Wang. (2021). Structural, morphological and transport properties of Ni doped ZnO thin films deposited by thermal co-evaporation method. *Materials Science in Semiconductor Processing*. 123: 105530.
- [22] P. Narin, E. Kutlu-Narin, S. Kayral, R. Tulek, S. Gokden, A. Teke, & S. B. Lisesivdin. (2022). Morphological and optical characterizations of different ZnO nanostructures grown by mist-CVD. *Journal of Luminescence*. 251: 119158.
- [23] M. Bai, M. Chen, X. Li, & Q. Wang. (2022). One-step CVD growth of ZnO nanorod/SnO₂ film heterojunction for NO₂ gas sensor. *Sensors and Actuators B: Chemical*. 373: 132738.
- [24] R. Ebrahimifard, H. Abdizadeh, & M. R. Golobostanfard. (2020). Controlling the extremely preferred orientation texturing of sol-gel derived ZnO thin films with sol and heat treatment parameters. *Journal of Sol-Gel Science and Technology*. 93: 28-35.
- [25] T. Amakali, L. Daniel, V. Uahengo, N. Y. Dzade, & N. H. De Leeuw. (2020). Structural and optical properties of ZnO thin films prepared by molecular precursor and sol-gel methods. *Crystals*. 10 (2): 132.
- [26] C. V. Manzano, L. Philippe, & A. Serrà. (2022). Recent progress in the electrochemical deposition of ZnO nanowires: Synthesis approaches and applications. *Critical Reviews in Solid State and Materials Sciences*. 47 (5): 772-805.
- [27] G. Zou, H. Li, Y. Zhang, K. Xiong, & Y. Qian. (2006). Solvothermal/hydrothermal route to semiconductor nanowires. *Nanotechnology*. 17 (11): S313.
- [28] S. Zhao, Y. Shen, X. Yan, P. Zhou, Y. Yin, R. Lu, ... & D. Wei. (2019). Complex-surfactant-assisted hydrothermal synthesis of one-dimensional ZnO nanorods for high-performance ethanol gas sensor. *Sensors and Actuators B: Chemical*. 286: 501-511.
- [29] P. Basnet, & S. Chatterjee. (2020). Structure-directing property and growth mechanism induced by capping agents in nanostructured ZnO during hydrothermal synthesis—A systematic review. *Nano-Structures & Nano-Objects*. 22: 100426.
- [30] M. N. I. Ghazali, M. A. Izmi, S. N. A. Mustaffa, S. Abubakar, M. Husham, S. Sagadevan, & S. Paiman. (2021). A comparative approach on One-Dimensional ZnO nanowires for morphological and structural properties. *Journal of Crystal Growth*. 558: 125997.
- [31] R. T. Hitchcock. (2004). Radio-frequency and microwave radiation. *AIHA*.
- [32] M. Vollmer. (2004). Physics of the microwave oven. *Physics Education*. 39 (1): 74.
- [33] A. Kumar, Y. Kuang, Z. Liang, & X. Sun. (2020). Microwave chemistry, recent advancements, and eco-friendly microwave-assisted synthesis of nanoarchitectures and their applications: A review. *Materials Today Nano*. 11: 100076.
- [34] C. Mallikarjunaswamy, V. Lakshmi Ranganatha, R. Ramu, Udayabhanu, & G. Nagaraju. (2020). Facile microwave-assisted green synthesis of ZnO nanoparticles: application to photodegradation, antibacterial and antioxidant. *Journal of Materials Science: Materials in Electronics*. 31: 1004-1021.
- [35] N. Devi, S. Sahoo, R. Kumar, & R. K. Singh. (2021). A review of the microwave-assisted synthesis of carbon nanomaterials, metal oxides/hydroxides and their composites for energy storage applications. *Nanoscale*. 13 (27): 11679-11711.
- [36] N. Garino, T. Limongi, B. Dumontel, M. Canta, L. Racca, M. Laurenti, ... & V. Cauda. (2019). A microwave-assisted synthesis of zinc oxide nanocrystals finely tuned for biological applications. *Nanomaterials*. 9 (2): 212.
- [37] K. J. Rao, B. Vaidhyanathan, M. Ganguli, & P. A. Ramakrishnan. (1999). Synthesis of inorganic solids using microwaves. *Chemistry of materials*. 11 (4): 882-895.
- [38] B. D. Cullity. (1956). *Elements of X-ray Diffraction*. Addison-Wesley Publishing.
- [39] H. M. Kingston and S. J. Haswell. (1997). Overview of microwave-assisted sample preparation. *Microwave Enhanced Chemistry: Fundamentals, Sample Preparation and Applications*. American Chemical Society, Washington DC. 55-222.
- [40] Y. He. (2004). Synthesis of ZnO nanoparticles with narrow size distribution under pulsed microwave heating. *China Particuology*. 2 (4): 168-170.
- [41] O. Palchik, J. Zhu, & A. Gedanken. (2000). Microwave assisted preparation of binary oxide nanoparticles. *Journal of Materials Chemistry*. 10 (5): 1251-1254.
- [42] S. Horikoshi, R. F. Schiffmann, J. Fukushima, & N. Serpone. (2018). Microwave chemical and materials processing. In *Microwave Chemical and Materials Processing* (pp. 33-45). Springer Singapore, Singapore.
- [43] M. H. Mamat, M. Z. Sahdan, Z. Khusaimi, A. Z. Ahmed, S. Abdullah, & M. Rusop. (2010). Influence of doping concentrations on the aluminum doped zinc oxide thin films properties for ultraviolet photoconductive sensor applications. *Optical materials*. 32 (6): 696-699.
- [44] M. F. Malek, M. H. Mamat, M. Z. Musa, T. Soga, S. A. Rahman, S. A. Alrokayan, ... & M. Rusop. (2015). Metamorphosis of strain/stress on optical band gap energy of ZAO thin films via manipulation of thermal annealing process. *Journal of Luminescence*. 160: 165-175.
- [45] X. Ge, K. Hong, J. Zhang, L. Liu, & M. Xu. (2015). A controllable microwave-assisted hydrothermal method to synthesize ZnO nanowire arrays as recyclable photocatalyst. *Materials Letters*. 139: 119-121.

- [46] A. U. H. S. Rana, & H. S. Kim. (2018). Growth condition-oriented defect engineering for changes in Au–ZnO contact behavior from Schottky to Ohmic and vice versa. *Nanomaterials*. 8 (12): 980.
- [47] R. A. Rani, A. S. Zoolfakar, W. S. W. M. Sabri, S. Alrokayan, H. A. Khan, & M. Rusop. (2018, June). Influence of the precursor and annealing temperature on the hydrothermal growth of ZnO nanostructures. In *IOP Conference Series: Materials Science and Engineering* (Vol. 380, No. 1, p. 012018). IOP Publishing.
- [48] O. Singh, N. Kohli, & R. C. Singh. (2013). Precursor controlled morphology of zinc oxide and its sensing behaviour. *Sensors and Actuators B: Chemical*. 178: 149-154.
- [49] R. Wahab, S. G. Ansari, Y. S. Kim, M. Song, & H. S. Shin. (2009). The role of pH variation on the growth of zinc oxide nanostructures. *Applied Surface Science*. 255 (9): 4891-4896.
- [50] M. C. Akgun, A. Afal, & H. E. Unalan. (2012). Hydrothermal zinc oxide nanowire growth with different zinc salts. *Journal of Materials Research*. 27 (18): 2401-2407.
- [51] K. P. Sridevi, S. Sivakumar, & K. Saravanan. (2021). Synthesis and Characterizations of Zinc Oxide Nanoparticles Using Various Precursors. *Annals of the Romanian Society for Cell Biology*. 8679-8689.